

Research Article pubs.acs.org/chemneuro

# Differential Interaction of Cannabidiol with Biomembranes **Dependent on Cholesterol Concentration**

Escarlin Perez, Jasmin Ceja-Vega, Michael Krmic, Alondra Gamez Hernandez, Jamie Gudyka, Riley Porteus, and Sunghee Lee\*



Cite This: ACS Chem. Neurosci. 2022, 13, 1046-1054



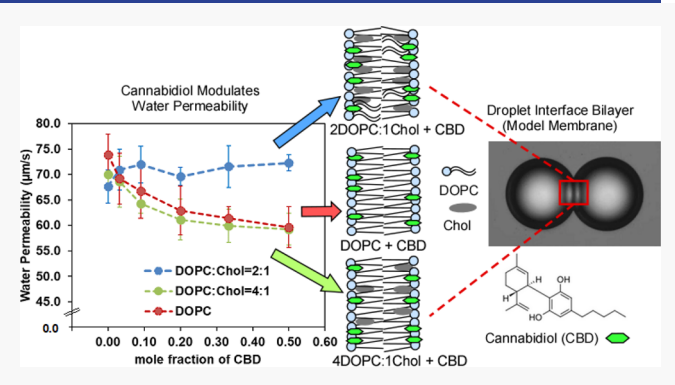
**ACCESS** 

Metrics & More

Article Recommendations

Supporting Information

ABSTRACT: Cannabidiol (CBD), the major nonpsychoactive component of plant-derived cannabinoids, has been reported to have a broad range of potential beneficial pharmacological effects on the central nervous system (CNS). In this study, the droplet interface bilayer, a model cell membrane, is used to examine the effects of CBD on passive water permeability, a fundamental membrane biophysical property. The presence of CBD decreases the water permeability of model lipid membranes composed of 1,2dioleoyl-sn-glycero-3-phosphocholine (DOPC) and at low concentrations of cholesterol (Chol) (20 mol %) in DOPC, whereas when higher concentrations of Chol are present (33 mol %), CBD has an opposing effect, increasing water permeability. The diametric effect in water permeability change upon addition of



CBD to Chol-low and Chol-high bilayers signifies a variant interaction of CBD, depending on the initial state of bilayer packing and fluidity. Additionally, differential scanning calorimetry studies provide evidence that there are selective changes in thermotropic behavior for CBD with DOPC and with DOPC/Chol membranes, respectively, supportive of these varying membrane interactions of CBD dependent upon cholesterol. The intriguing ability of CBD to sensitively respond to membrane Chol concentrations in modifying physical properties highlights the significant impact that CBD can have on heterogeneous biomembranes including those of the CNS, the neurons of which are enriched in Chol to a point where up to a quarter of the body's total Chol is in the brain, and defective brain Chol homeostasis is implicated in neurodegenerative diseases.

KEYWORDS: cannabidiol (CBD), model membrane, cholesterol, water permeability, differential scanning calorimetry

## INTRODUCTION

Cannabidiol (CBD), the major nonpsychoactive component of Cannabis sativa and naturally present in Cannabis plants, has gained increasing notability for its perceived potential health benefits. Many existing studies focus on the elucidation of the biopharmaceutical characteristics and effects of CBD and specific molecular targets with which it interacts, 2,3 as well as on enhancing its bioavailability through diverse drug delivery formulations to overcome the intrinsic limitations of the CBD molecule (low water solubility, 12.6 mg/L) for future therapeutic applications.4 CBD has been reported to have a broad range of potential beneficial pharmacological effects on the central nervous system, including indications for epilepsy and chronic pain. In a placebo-controlled trial of CBD in schizophrenia, treatment that was adjunctive to antipsychotic medicaments was significantly associated with positive psychotic symptoms.<sup>6</sup> Additionally, CBD was shown to protect against amyloid- $\beta$ -induced insults and has a variety of other neuroprotective effects.7 Furthermore, there is evidence for anti-inflammatory, antioxidant, antimicrobial, antiproliferative, and pro-apoptotic effects on various cancer types.  $^{8-11}$  CBD has low affinity for CB-type cannabinoid receptors, and so therefore, the pharmacological activity of CBD has been linked to a wide variety of CB-independent molecular targets including ion channels, enzymes, transporters, and receptors. 12,13 However, its specific molecular pharmacological mechanism of action, including direct mode of interaction with claimed molecular targets, is not fully understood. Considering the fact that many of the molecular targets implicated are membrane-bound, combined with the highly lipophilic nature of CBD (logP value estimated at ca. 6.5), 14 it has been suggested that CBD-induced changes in diverse membrane-associated targets can occur as a result of changes in the physicochemical properties of the neighboring lipid bilayer and membrane heterogeneities via nonspecific inter-

Received: January 15, 2022 Accepted: March 8, 2022 Published: March 17, 2022





actions.<sup>15</sup> For example, in a recent study, CBD has been shown to alter membrane elasticity in such a way to contribute to the inhibition of the voltage-gated sodium channel Nav1.4, channels which initiate neuronal action potentials with Na ion current.<sup>16</sup> This result would be consistent with the burgeoning conceptual acceptance that the collective structure and physical properties (e.g., membrane elasticity, thickness, and area per lipid headgroup) of lipid bilayers can play a critical role in the physiological activity of membrane proteins.<sup>17–19</sup> However, relatively fewer studies have presented evidence demonstrating a capacity of CBD to directly modulate the physicochemical properties of membrane bilayers.<sup>20–23</sup>

Cholesterol (Chol) plays a crucial role as a major component of the plasma membrane, comprising a high fraction of total lipid (ca. 20 to 50 mol %). The major role of Chol in the membrane is its organizing effect upon other lipidic components of the membrane, to thereby modulate the structural and physicochemical properties of the plasma membrane lipid bilayer and, as a result, regulate the function of a wide range of transmembrane proteins. 24-26 This sterol has an especially high prevalence in the brain, the most cholesterol-rich organ of the body, having 20% of all body cholesterol.<sup>27</sup> Chol has been reported to regulate cannabinoid enhancement of GlyR (glycine receptors) function, suggesting that Chol is critical for the cannabinoid-GlyR interaction in the cell membrane.<sup>28</sup> A system-level analysis of CBD action in human cell lines using temporal multiomic profiling has been reported to evince CBD's ability to perturb Chol-dependent membrane properties and disrupt Chol homeostasis pathways.<sup>29,30</sup> It has also been suggested that CBD and Chol may bind to the same site on transmembrane proteins based on shared activity at multiple targets, through direct binding and nonspecific interactions for both CBD and Chol.<sup>29</sup> Chol is also a key component of lipid rafts, considered the major platforms for signaling regulation.<sup>31</sup> In the brain, lipid rafts are seen to contribute to the clustering of neurotransmitter receptors and concomitant effects on neuronal communication. 32,3

The composition of various cell membranes is very complex, including an extensive variety of lipids, carbohydrates, and proteins.<sup>34</sup> Due to the complexity of cellular biological membranes, model lipid membranes have been proposed as useful platforms to gain insight into the role of lipids in drugmembrane interactions in a defined and controlled way. 35 One such model membrane includes the droplet interface bilayer (DIB), constructed by bringing into contact two individual aqueous droplets bounded by lipid in a surrounding oil medium, to create a bilayer region. The region adopts a structure essentially the same as the double leaflet lipid bilayer structure of cellular plasma membranes, as shown in Figure 1.36,37 The lipid bilayer in a DIB membrane generally adopts the lamellar phase (e.g.,  $L_d$ , liquid disordered). The versatility of DIB membranes has found many new uses, including the study of bioelectric phenomena, 40 transmembrane transport,41 mechanotransduction,42 3D printing of model tissue, <sup>43</sup> and crystallization, <sup>44</sup> among many others.

In our earlier studies, we have demonstrated that a DIB

In our earlier studies, we have demonstrated that a DIB provides a convenient and reliable system for investigating membrane water transport phenomena, which finds its importance for understanding the passive transport of water molecules across bilayer membranes, a phenomenon that plays a significant role in understanding cellular physiology and maintaining homeostasis, and is of considerable importance for

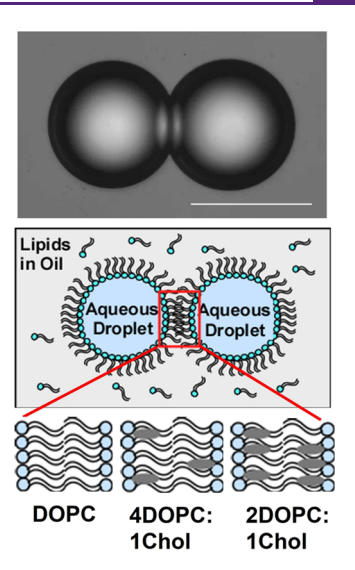


**Figure 1.** Droplet interface bilayer (DIB) is formed by bringing into contact apposed lipid-coated aqueous droplets to form a bilayer when these droplets are brought together in an immiscible oil medium, forming a membrane-mimetic structure consisting of a double leaflet of lipids organized into a lipid bilayer structure. Bilayers were composed, respectively, of DOPC, 4DOPC/1Chol, and 2DOPC/1Chol. The scale bar on the videomicrograph represents 100  $\mu$ m.

the overall functioning of the cellular plasma membrane.<sup>47</sup> However, the transport of hydrophilic species such as ions and protons usually also involves water; that is, water penetration assists these hydrophilic moieties to permeate the lipid membrane. Therefore, water permeability has been suggested to constitute a measure to assay membrane stability for ionic leakage. 48 There is also a need to improve understanding of transmembrane fluid transport in the brain as well, in order to better develop pharmacological remedies for diseases of impaired homeostasis of brain fluids, such as edema and hydrocephalus. 49 Given that the water transport process is a function of the underlying physical state of the lipid bilayer and its structure, 50 it has been desirable to establish a consistent and reliable platform for quantifying water transport through bilayers, as a means to shed light on bilayer physical properties. Toward this, our previous findings provide ample demonstration of how self-assembly of lipidic amphiphiles at the interdroplet interface serves to provide flexible levers for probing structural effects, 51-54 including exploration of the effects of exogenous molecules on membrane properties.<sup>55</sup>

In this study, we have assembled three compositionally different DIB-based biomimetic membranes of varying Chol concentrations and investigated the role played by CBD in the dynamic properties of these model membranes. Changes in the membrane dynamics will have potential consequences upon the transport phenomena of lipid membranes. As the basic component of a DIB model membrane, we used a neutral zwitterionic ester-linked glycerophosphocholine lipid commonly found in eukaryotic cell membranes, namely, 1,2dioleoyl-sn-glycero-3-phosphocholine (DOPC). This lipid plausibly has a significant presence in neuronal cells, based on computational lipidomics of the brain membrane that indicate an average number of unsaturations per lipid tail of between 0.90 and 1.63 (dependent on the leaflet), and a fraction of up to 0.25 phosphatidylcholine in the outer leaflet.<sup>56</sup> We also used two different mixtures of DOPC with Chol (4:1 and 2:1, mole ratios of DOPC/Chol, respectively)

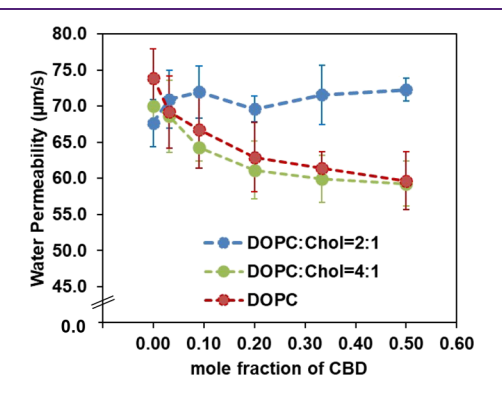
to represent a membrane providing a more complex biomimetic composition. CBD, shown in Figure 2, is

Figure 2. Structure of cannabidiol (CBD).

composed of a pentyl-substituted bis-phenol aromatic group linked to an alkyl-substituted cyclohexene terpenic ring system, which renders it highly lipophilic, a characteristic associated with the rapid transfer of CBD across the blood—brain barrier, for example. <sup>57</sup>

#### RESULTS AND DISCUSSION

Effects of Cannabidiol on the Water Permeability of Model Membranes: DOPC, 4DOPC/1Chol, and 2DOPC/1Chol. Figure 3 displays the osmotic water permeability



**Figure 3.** Osmotic water permeability coefficients ( $\mu$ m/s) of the lipid bilayer formed from DOPC, 4DOPC/1Chol, and 2DOPC/1Chol, at 30 °C with varying mole fractions of CBD. Each data point represents an average of individual permeability runs ( $n \ge 50$ ), and standard deviation as error bars.

coefficients ( $P_c$ ) of DOPC-based membranes at 30 °C (one composed of DOPC, another of a 4:1 molar ratio of DOPC/ Chol, and another being 2:1 DOPC/Chol) as a function of varying mole fractions of CBD in the lipid mix. The corresponding permeability coefficients are shown in Table S1 (Supporting Information). The results indicate that the change in water permeability induced by CBD differs, depending on the nature of the lipid components and concentration of CBD. As shown in Figure 3, the  $P_f$  values for water transport across DOPC membranes (red circles) decrease with the increasing concentration of CBD. The abscissa denotes the mole fraction of CBD as a proportion of total lipid + CBD. Specifically, on comparing P<sub>f</sub> values for DOPC lipid bilayers containing the lowest level of CBD we employed (i.e., at a 30:1 DOPC/CBD mole ratio) and those of the control DIB formed from DOPC, an approximately 6% decrease in water permeability (from 73.8 to 69.2  $\mu$ m/s) was observed. The decrease in water permeability is further enhanced with the increasing concentration of CBD, attaining 59.7  $\mu$ m/s at a 1:1 DOPC/CBD mole ratio (0.50 mole fraction CBD), i.e., a 19% decrease from the  $P_f$  of the DIB formed from DOPC at the same temperature.

Although CBD is not typically introduced into organisms in pharmacological doses that obtain plasma concentrations of nearly equimolar CBD to organismal lipid (as used here), there is a tendency for drug molecules to accumulate at lipid interfaces, leading to the local concentration of drug in the interfacial region being much greater than the global concentration. S8

As a control, we explored the effect of Chol alone on DOPC transport properties. In the absence of CBD, introduction of Chol into a DOPC DIB membrane progressively reduces observed water permeability  $P_f$  from 73.8  $\mu$ m/s for DOPC to 70.0  $\mu$ m/s (for 4:1 DOPC/Chol) and to 67.7  $\mu$ m/s (for 2:1 DOPC/Chol). The decrease in water permeability with the increasing concentration of Chol is consistent with the known condensing effect of Chol in lipid bilayers. As is known, the inclusion of Chol tends to stiffen fluidic membranes and will reduce permeation. Increasing the amounts of Chol in DOPC membranes has been reported to cause a corresponding decrease in area occupied by the lipid and also corresponds to a decrease in water permeability across these membranes.<sup>59</sup> The condensing effect of cholesterol in DOPC lipid bilayers was also reported via atomistic molecular dynamics simulation for a mole fraction of up to 0.66 at 323 K.60 In the Chol ranges we studied, the Chol concentration was below the solubility limit in DOPC, as evidenced by reports that DOPC-Chol mixtures do not exhibit phase separation at mole fractions of 0.25 and 0.5.61 In addition, they behave as an ideal solution, with surface area per lipid having a near-linear decrement with increasing Chol concentrations.

Subsequently, we investigated the water permeability values for two different mole ratios of DOPC/Chol (namely, 4:1 and 2:1), as they each experience varying concentrations of CBD. The range for the ratio of total lipid to CBD was from 30:1 to 1:1 mol/mol. As seen in Figure 3, with the increasing concentration of CBD in the 4:1 DOPC/Chol bilayer, the change in water permeability followed a trend similar to that of DOPC, i.e., a decrease in water permeability with the increasing concentration of CBD. When Chol is incorporated into the DOPC membrane at a higher concentration (2:1 DOPC/Chol mole ratio), there is no significant decrease in water permeability as a function of CBD inclusion. In fact, there is a seemingly slightly higher water permeability than in the absence of CBD. This observation is a sharp contrast to the scenario of the DOPC bilayer, as well as the low concentration of Chol, where, in each case, the water permeability gradually decreased with the increasing CBD concentration.

Previous observations in the literature indicate that the hydrocarbon chain regions of the lipid bilayer environment are sensitive to interaction with CBD, presumably owing to the lipophilic nature of the latter. Through electron spin resonance studies on a spin-labeled liposome bilayer, CBD has been shown to increase the molecular order (rigidity) in lecithin/ Chol liposomes (1.0:0.9 mole ratio) at CBD molar ratios of 20 total lipid/1 CBD or less.<sup>20</sup> In recent studies by Ghovanloo et al., 13 CBD is reported to inhibit the skeletal muscle Nav1.4 ion channel indirectly by alterations in membrane elasticity, suggestive of increases in membrane stiffness, as well as directly blocking the Nav1.4 ion channel. In addition, the effect of CBD on the polarization of fluorescence of probe molecules (1,6-diphenyl-1,3,5-hexatriene (DPH)) in synaptic plasma membranes showed a significant increase of DPH fluorescence polarization at micromolar concentrations, indicative of an ordering effect on the membrane.<sup>23</sup> In the latter study, the

change in DPH mobility produced by CBD is dependent upon the degree of initial bilayer order, where CBD increased DPH fluorescence polarization in unsaturated and fluidic membranes (C16:1), while decreased fluorescence polarization of DPH was seen in more rigid and saturated PC, such as DMPC (C14:0) and dipalmitoyl phosphocholine (DPPC) (C16:0). Similarly, egg PC also shows an increase in DPH polarization upon interaction with CBD but a decrease in polarization for Chol-containing egg PC (2:1, PC/Chol).<sup>23</sup> NMR studies on the interactions of CBD with model membranes of egg yolk lecithin/Chol showed that CBD increases the restriction of molecular motions of the hydrocarbon chains when the membrane contains cholesterol.<sup>22</sup>

In general, water permeability has been shown to be dependent on the physical properties of individual lipids and their aggregate bilayers, such as thickness, fluidity/rigidity, and area per molecule. 59,63 Overall, fluidity/rigidity in bilayers is generally correlated with the packing density of lipids, 64 and water permeability is indeed expected to depend on the lipid packing in the bilayer region. Our findings, which show the evident decrease in the water permeability coefficient for membranes containing progressively increasing quantities of CBD in the cases of DOPC and of DOPC with Chol (at a 4:1 DOPC/Chol mole ratio), are consistent with the previous reports indicating the rigidifying effect of CBD on fluidic model membranes. The diametric effects in water permeability change upon addition of CBD to Chol-low and Chol-high bilayers, seen here, are also consistent with the earlier reported studies signifying a differential effect of CBD depending on the initial state of bilayer packing and fluidity.

Effects of Cannabidiol on the Thermotropic Properties of DOPC, 4DOPC/1Chol, and 2DOPC/1Chol Model Membranes. We sought to ascertain the effect of CBD on the thermotropic properties of the multilamellar vesicles of DOPC and of DOPC/Chol. The endothermic differential scanning calorimetry (DSC) thermograms for these multilamellar vesicles in the presence of different concentrations of CBD are shown in Figure 4, and the corresponding thermodynamic

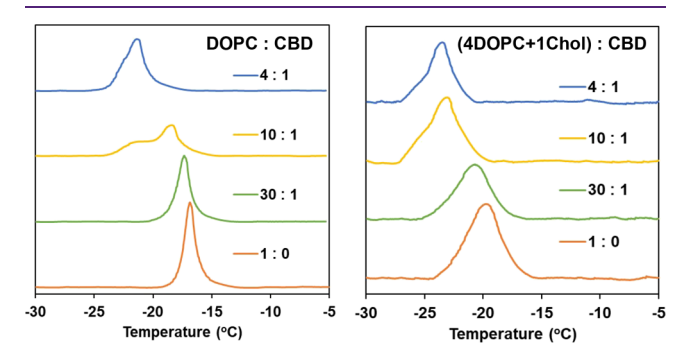


**Figure 4.** Endothermic calorimetric thermograms of multilamellar vesicles of (A) DOPC and (B) 4DOPC/1Chol containing CBD; from bottom to top in the mole ratio of lipid (lipid mixture)/CBD: (orange) 1:0, (green) 30 total lipid/1 CBD, (yellow) 10 total lipid/1 CBD, and (blue) 4 total lipid/1 CBD.

data are shown in Table 1. The thermogram of the DOPC multilamellar vesicle exhibits well-defined endothermic transitions, arising from the conversion of the lamellar gel phase,  $L_{\beta}$ , to the lamellar liquid-crystalline state,  $L_{\alpha}$ , at the temperature  $T_{\rm m} = -16.8$  °C, with a melting enthalpy of 36.69 kJ/mol. The DSC characteristics of phase transition for

Table 1. Temperature  $(T_{\rm m})$  and Enthalpy  $(\Delta H)$  for Phase Transition of Multilamellar Vesicles of Different Compositions at Varying Concentrations of CBD

	DOPC		4DOPC/1Chol	
lipid: CBD (mol)	T <sub>m</sub> (°C)	$\Delta H$ (kJ/mol)	<i>T</i> <sub>m</sub> (°C)	$\Delta H$ (kJ/mol)
1:0	-16.8	$36.69 \pm 0.42$	-20.1	$13.97 \pm 0.63$
30:1	-17.4	$35.52 \pm 1.26$	-21.0	$9.58 \pm 0.84$
10:1	-18.5	$34.39 \pm 1.26$	-23.3	$12.18 \pm 0.84$
4:1	-21.4	$34.94 \pm 1.05$	-23.5	$9.75 \pm 0.63$

DOPC multilamellar vesicles are in agreement with literature data.  $^{65}$  The low  $T_{\rm m}$  value indicates that the DOPC membrane is in the disordered fluidic state due to the presence of double bonds in each hydrocarbon chain.

CBD interacts with DOPC bilayers and influences their thermotropic phase behavior in a concentration-dependent manner, as indicated by the significant effect on the thermogram (Figure 4A). Compared to DOPC, T<sub>m</sub> is decreased to -17.4 °C at a 30:1 total lipid/CBD mole ratio; this value was further decreased to -18.5 °C at a 10 to 1 mole ratio and -21.4 °C at a 4:1 mole ratio of total lipid/CBD. In addition, at a 10 to 1 mole ratio, a phase separation was observed, as indicated by the appearance of splitting of the peak into two components having different peak temperatures (at -18.5 and -21.4 °C). This splitting could be interpreted as arising from creation of a separate phase having uneven CBD distribution. An analogous phase separation exists in the literature for the DPPC vesicle bilayer: a splitting of the DSC phase transition for DPPC was seen at a 5 to 1 molar ratio of DPPC to CBD.<sup>21</sup> As the concentration of CBD increased to a 4:1 mole ratio (DOPC/CBD), there is a significant change in the thermogram. On comparing the thermogram of the 10:1 mole ratio to that of the 4:1 mole ratio, the high-temperature component (i.e., at -18.5 °C) of the 10:1 mole ratio trace has shifted to a lower temperature, almost merging with the lowtemperature component (which stays at -21.4 °C). The shoulder in the 4:1 mol ratio thermogram suggests some nonideal mixing. Table 1 summarizes these transition temperatures; however, for any split peaks, the temperature reported is only for the most intense peak. When enthalpy values for both phase transitions from twin peaks are combined (enthalpy data in Table 1 represent the total area for two peaks), there appears to be no dramatic change in the total enthalpy for the CBD concentration ranges studied, which could be indicative of an overall orderly arrangement within the hydrocarbon core of DOPC without disrupting the interior of the lipid bilayer. It is postulated here that CBD has a predominant population at the bilayer surface to interact via hydrogen bonding with the polar headgroups of the lipid primarily affecting the  $T_{\rm m}$ . An earlier study shows a similar effect: in DSC traces of CBD interacting with phospholipid vesicles, little change in the enthalpy of transition accompanies a significant lowering of  $T_{\rm m}$ . These data are consistent with previously posited general findings that molecules inserted into a lipid bilayer array as interstitial impurities (rather than substituting for lipid) will generally not affect enthalpic changes for the array even as they cause changes in  $T_{\rm m}$ .

For comparison, we analyzed the effect of Chol alone on the DOPC thermotropic properties, in the absence of CBD. The corresponding DSC thermograms for the binary lipid bilayers as a function of Chol content are shown in Figure S1 (Supporting Information). With the increasing concentration

of Chol, there is a shift toward lowering of the main phase transition temperature, together with a significant decrease in enthalpy. At a DOPC/Chol mole ratio of 2:1, the  $T_{\rm m}$  value displays a considerable shift of ca. -7 °C. The transition enthalpy is almost abolished at a mole ratio of 2:1 (and completely disappears at 1:1). These results are consistent with previous reports on DOPC bilayers as a function of cholesterol content. Since our results established that the high Chol case (i.e., 2:1 DOPC/Chol) does not have a well-defined enthalpic transition in DSC, but the 4:1 DOPC/Chol binary system does show such a peak, we chose to employ solely the 4:1 DOPC/Chol system to explore CBD interaction with the Chol-containing DOPC bilayer in our DSC studies.

The DSC thermograms of the ternary DOPC/Chol/CBD system are presented in Figure 4B (Table 1) as a function of increasing CBD concentration, for the case of DOPC/Chol (4:1 mole ratio). The highest concentration of CBD was 4:1 total lipid/CBD (termed as "high CBD limit"). In general, as the mole fraction of CBD in DOPC/Chol bilayers increases, the main transition peak is moved toward a lower temperature. Bilayers of DOPC/Chol show a  $T_{\rm m}$  shift, by 3.4 °C, as the CBD content in the bilayer is increased to the high CBD limit (Figure 4B). There appears to be a saturation effect in the lowering of  $T_{\rm m}$  values for DOPC/Chol; however, an initially marked decrease in  $T_{\rm m}$ , which is seen at up to 10:1 mole ratio total lipid/CBD, is leveled off at the high CBD limit. Starting at the 10:1 mole ratio of total lipid/CBD, a slight phase separation (peak shoulder) began to be apparent and was more pronounced at a 4:1 mole ratio. It is likely that one peak component is associated with the phase transition of lipid regions containing high amounts of CBD, while the other peak component is due to the phase transition of CBD-poor lipid regions. The enthalpy of transition gradually decreases (from a value of 13.97 kJ/mol in the absence of CBD) upon interaction with CBD, to about 9.75 kJ/mol at a high CBD limit, a significant decrease of about 30%. (This is in contrast to the Chol-free DOPC-CBD interaction, where no appreciable enthalpy changes were observed, and no more than 5% decrease in enthalpy at a high CBD limit was observed). In summary, there are differential changes in  $T_{\mathrm{m}}$  and  $\Delta H$  for CBD with DOPC and with DOPC/Chol membranes, respectively, indicative of varying membrane interactions of CBD dependent upon cholesterol.

Interestingly, our data show that inclusion of either CBD or Chol (separately) into DOPC bilayers, each lowers membrane water permeability. At the same mole concentrations of each, this effect is even greater for CBD as compared to Chol. Specifically, water permeability  $P_{\rm f}$  is reduced from 73.8 (DOPC) to 62.9  $\mu$ m/s (DOPC/CBD 4:1) vs 70.0  $\mu$ m/s (DOPC/Chol 4:1), and an analogous trend is obtained for the 2:1 mole ratio of phospholipid to either CBD or Chol, respectively. An ability of CBD to reduce water permeability may point to a membrane rigidifying effect for CBD in fluidic membranes, one brought about by areal condensation of the phospholipids surrounding CBD molecules to shield hydrocarbon portions of CBD from the aqueous interface, akin to the "umbrella effect" postulated to account for the cholesterol condensing effect in bilayers. 70 Also, with respect to the comparative thermotropic behavior of CBD and Chol in the DOPC array, it is Chol that markedly reduces the DOPC cooperativity when present at 20 mol %, but CBD does not reduce the cooperativity to the same extent. This is likely due to Chol interacting relatively more with the acyl chains of DOPC, whereas CBD locates closer to the DOPC headgroups. In addition, while Chol-containing DOPC bilayers show a nearly symmetric phase transition peak at concentrations we studied, the addition of CBD likely produces a phase separation at and above concentrations of 10:1 lipid to CBD. These findings are very timely, since in recent reports, <sup>30,71</sup> it was found that CBD increased the accessibility of membrane cholesterol to cholesterol oxidase and reduced the lateral diffusion of cholesterol. This was ascribed to partitioning of CBD into cellular membranes, leading to disruption of cholesterol-dependent membrane properties, manifesting in a marked pro-apoptotic effect in primary microglia. Our findings thus add to the intriguing and burgeoning interest in the interplay between Chol and CBD.

Additional insight into the interaction of CBD with the lipid bilayer can be deduced from studies related to the respective internal membrane stress profiles for the three lipidic systems. The pressure profile internal to a lipid bilayer arises from several factors, including (1) a tension in the direction perpendicular to the plane of the membrane, which creates a negative pressure at the interface between the polar headgroups and the hydrophobic tails, and (2) positive pressures that counterbalance the tension, created both by headgroup repulsion and by the unfavorable entropy of the hydrophobic tail region. Changes in this lateral pressure have long been hypothesized to induce activation of ion channels in general<sup>73,74</sup> and demonstrably so in the case of mechanosensitive channels. 75,76 The DIB system is capable of offering insight into such energetics for the lateral arrangement of lipids, particularly, the relative lateral pressure  $\pi_{i}^{55,77}$  which is a measure of the compaction of a single leaflet of the bilayer relative to its compaction at the water-oil interface. It is determined from the difference between the interfacial tension at the water/oil interface  $(\gamma_m)$  and the surface tension of a single bilayer leaflet of the same composition that  $\pi = \gamma_m$  –  $0.5\gamma_b$ , and it will be positive for any (meta)stable DIB.<sup>77</sup> Values of interfacial tension at the oil/water interface are amassed from droplet tensiometry, and bilayer tension  $\gamma_b$  is derived from Young-Dupré balance of forces between droplets that adhere at a bilayer:  $\gamma_{\rm b} = 2\gamma_{\rm m}(\cos\,\theta)$ , where  $\theta$  is the contact angle between the droplets.<sup>78</sup> For the DOPC bilayer, the relative membrane lateral pressure is 0.13 mN/m, which is decreased to 0.11 mN/m upon inclusion of the 1:1 mole ratio of CBD. For a bilayer that contains Chol (DOPC/Chol at a 4:1 mole ratio), the decrease in relative lateral pressure is more modest: from a value of 0.10 mN/m in the absence of CBD to 0.09 mN/m (in the presence of total lipid/CBD of a 1:1 mole ratio). However, when the presence of Chol is increased (DOPC/Chol at a 2:1 mole ratio), there are negligible relative lateral pressure changes upon inclusion of total lipid/CBD of a 1:1 mole ratio. It is to be noted that while  $\pi$  is merely a relative lateral pressure (difference between monolayer and bilayer packing) and represents a parameter for overall packing in the aggregate of the bilayer and not internal gradients of lateral pressure within the bilayer, it can be considered useful to quantify the effect of bioactive molecules on lipid order. These data, indicating a relative insensitivity in relative lateral pressure changes to the presence of CBD molecules when the membrane contains high cholesterol, comport with our observation that there is no appreciable change in membrane water permeability upon interaction of CBD with the cholesterol-containing bilayer.

ACS Chemical Neuroscience pubs.acs.org/chemneuro Research Article

Combined results from water permeability and thermotropic property studies suggest that CBD molecules may exert an effect on phospholipid bilayers in reducing the mobility of the hydrocarbon chains in phospholipid bilayers and influencing hydrocarbon chain cooperativity, depending on initial state of bilayer fluidity. When the phospholipid molecules are relatively loosely packed (as in the DOPC bilayer, or in DOPC bilayers having only low concentrations of Chol, e.g., 4:1 DOPC/ Chol), the array would have sufficient initial flexibility to accommodate partitioning of CBD molecules into the bilayer. However, in more ordered lamellas such as in the case of high concentrations of Chol (e.g., 2:1 DOPC/Chol), the extent of CBD penetration into the hydrocarbon chain may become limited due to the rigidifying effect of Chol on the fluidic DOPC membrane. If CBD cannot penetrate, then polar interactions will maintain CBD molecules at the interfacial region of the phospholipid palisade. Competition between CBD and Chol, the latter also anchored at the interface, might perturb the orientation of Chol molecules and compromise their ordering ability, which is reflected in our observation of a slightly increased water permeability. It is also possible that competition between CBD and Chol may exist in the hydrophobic core as well. Such CBD interaction would also perturb the phospholipid hydrocarbon chains and decrease the  $T_{\rm m}$  value and decrease  $\Delta H$  as evidenced by our DSC study. Figure 5 schematically depicts the various effects of CBD.

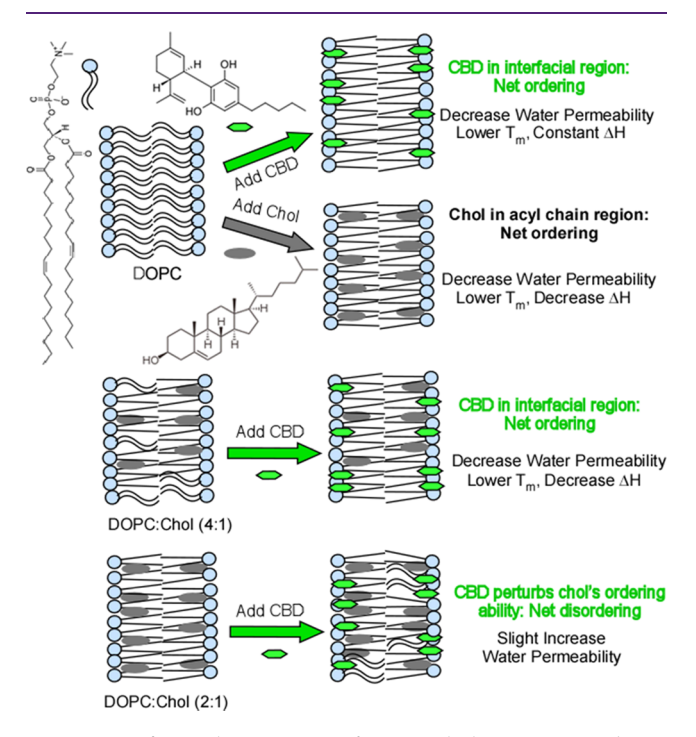


**Figure 5.** Differential interactions of CBD with the DOPC membrane with varying Chol concentrations.

# CONCLUSIONS

In this study, we have investigated the interplay among CBD, Chol, and a representative neuronal phospholipid in a biomimetic membrane array, from the standpoint of two vital biophysical properties: passive transbilayer transport and thermotropic behavior. Three compositionally different model biomimetic membranes were explored, using the flexibility of the self-assembled bilayer structure of the interdroplet

interface. Our data show that CBD, a neuroactive derivative of Cannabis with reported antiseizure properties, induces water permeability reduction, indicating the rigidification of lipid bilayers composed of DOPC bilayers. Notably, the extent of ordering can be enhanced in the presence of low amounts of Chol in the membrane (4:1 mole ratios of DOPC/Chol), while at high concentrations of Chol (2:1 mole ratios of DOPC/Chol), the effect is the opposite. We find a sensitive and differential ability for CBD to interact with the lipid bilayer, dependent on the membrane Chol concentration, and to modify the biophysical properties of model membranes. These results highlight the significant interplay between CBD and membranes containing Chol, a major brain membrane component. Such phenomena provide useful insight into the interaction of CBD with membranes in a heterogeneous environment and into the understanding of the nonspecific effects of CBD having significant functional consequences, such as influence upon membrane protein activity. It is recognized that the neuronal cell membrane has a wide variety of lipid components, including not just cholesterol in large quantities but also all major lipidic classes and up to 49 different kinds of lipids, all of which in the aggregate affect the biophysical properties of the neuronal bilayer.<sup>79</sup> Thus, this diversity will inform the context of our future work in which CBD (among other neuroactive phytochemicals) will be studied with even more sophisticated models to elucidate the fundamental interactions underpinning their neurological impact, since further exploration of the interaction of CBD with the various components of the cellular membrane is sorely needed to understand and achieve its therapeutic potential.

### EXPERIMENTAL METHODS

Materials and Sample Preparations. Lipids used in the current study were obtained from Avanti Polar Lipids, Inc. (Alabaster, AL) with 99+ % purity and used as received without further purification. DOPC was provided as a solution in chloroform, a solvent readily removable by high vacuum or stream of inert gas. Squalene (2,6,10,15,19,23-hexamethyl-2,6,10,14,18,22-tetracosahexaene;  $C_{30}H_{50}$ ; "SqE") was used as the immiscible organic phase in DIB experiments (and is chosen since its large molecular size ensure that it is largely excluded from being present within the lipid bilayer), and all other chemicals, including cholesterol (Chol) and cannabidiol (CBD), were of the highest purity available and were purchased from Sigma-Aldrich and used without additional purification. SqE is elected as an immiscible phase since its molecules are excluded from the DIB bilayer due to their large molecular size, to form an essentially solvent-free DIB. All lipid and Chol samples were stored at −20 °C until use and freshly prepared immediately before use in experiments. Pure SqE was stored in the temperature range of 2–8 °C. Cholesterol was delivered to the bilayer via a homogeneous bulk oil solution containing DOPC and cholesterol at a molar ratio, from 4:1 to 2:1. In order to prepare an oil solution containing DOPC (with or without Chol), a chloroform solution of DOPC (optionally with Chol) can be evaporated under inert gas to make a dried thin film of lipid (or the lipid mixture) followed by overnight vacuum drying for complete removal of any residual solvent. When CBD is used, it is codissolved with the lipid or lipid mixture. The appropriate amount of CBD (acquired as 1 mg/mL methanolic solution) is codissolved with lipid (or the lipid mixture with Chol) in chloroform followed by the complete evaporation of the solvent to generate a dried CBD/lipid film of a defined molar ratio of lipid to CBD. For water permeability experiments, such a dried CBD/lipid film is then dissolved in SqE, to a total lipid concentration of 5 mg/mL. For sample preparations used in DSC, a suspension of multilamellar liposomes was obtained as follows: the dried CBD/lipid film described above is subsequently rehydrated with aqueous solution, to a total lipid concentration of ca.

16 mg/mL, and then vortexed for about 5 min followed by bath sonication of ca. 30 min. Further treatment with seven freeze—thaw cycles using liquid nitrogen did not influence phase behavior shown in DSC. Aqueous solutions containing osmolytes (NaCl at nominally 0.1 M) were prepared from deionized water (18.2 M $\Omega$ ·cm) purified in a Millipore water purification system (Direct Q-3). The osmolality (in mOsm/kg) of all aqueous solutions used was measured with a vapor pressure osmometer (VAPRO model 5600) immediately after fresh preparation of each solution, as well as prior to use.

Extraction of Water Permeability Transport Parameters across the Droplet Interface Bilayer (DIB). The water permeability measurements were performed using the model membrane obtained by the DIB protocol. The detailed experimental setup and full procedure have been described elsewhere. 52 In brief, a pair of osmotically unbalanced aqueous droplets, one typically being a pure water and the other being a droplet of 0.1 M NaCl, each having approximately 100  $\mu$ m diameter, are dispensed from a micropipette into squalene (SqE) solvent, which contains lipid or lipid mixtures and then brought into contact, and consequent volume changes are derived from videomicrographic observation. All water permeability experiments were carried out at 30 °C, using a custom-built temperature-controlled microchamber, which was thermostatted via an external circulating water bath. The temperature of the microchamber containing lipid mixtures is measured by thermocouple wire and is accurate to  $\pm 0.1$  °C. When the two osmotically unbalanced microdroplets, each covered with lipid, were made to adhere at a bilayer, osmotic water transport immediately commenced through the bilayer (contact zone), resulting in a visible change in the droplet diameter. The osmotic gradient drives water transport through the droplet bilayer. Any electrolyte flux is expected to be negligible compared to that of water, since ion permeation is typically almost eight orders of magnitude slower than that of water. 80 Changes in droplet size due to this water transport were thus measured from the commencement of the process. The detailed method of the determination of the water permeability coefficient is provided in the Supporting Information.

Differential Scanning Calorimetry. Thermal phase transition study was performed with a TA Q2000 differential scanning calorimeter and analyzed using TA Universal Analysis software for the main phase transition behavior of the samples. The main phase transition temperature used here,  $T_{\rm m}$ , corresponds to the temperature at the apex of the endothermic transition peak. The phase transition enthalpy was obtained by integrating the area under the heat capacity curve. A sample (ca. 15  $\mu$ L) of the multilamellar vesicle suspension prepared described above was hermetically sealed, heated, and cooled at rates of 5 °C/min. Reported values are determined from two to three different samples. Each sample was cycled three times to check if there is any hysteresis, and in all cases, reproducible results were obtained on consecutive heating and cooling cycles.

Interfacial Tension and Contact Angle Measurement. The interfacial (oil—water) tension was measured with a ramé-hart advanced goniometer/tensiometer (Model 590) in conjunction with image analysis software DROPImage. Typically, ~2 mL of an aqueous phase (0.1 M NaCl) was used, into which was introduced a pendent drop of an oil phase containing DOPC or DOPC with Chol (with varying mole ratios of CBD) having a volume of <1  $\mu$ L. For the contact angle ( $\theta$ ) measurement, two apposing iso-osmotic droplets are brought into proximity using two micropipettes and then touched together to make contact with each other. The method of the determination of the contact angle from the microscopic images is provided in the Supporting Information.

#### ASSOCIATED CONTENT

# Supporting Information

The Supporting Information is available free of charge at https://pubs.acs.org/doi/10.1021/acschemneuro.2c00040.

The method of the determination of water permeability coefficients; the osmotic water permeability of DOPCbased membranes as a function of varying mole fractions of CBD in the lipid mix; DSC thermograms for the binary DOPC bilayer as a function of Chol content; and the method of the determination of the contact angle from the microscopic image (PDF)

#### AUTHOR INFORMATION

#### **Corresponding Author**

Sunghee Lee — Department of Chemistry and Biochemistry, Iona College, New Rochelle, New York 10801, United States; orcid.org/0000-0003-2481-7982; Phone: 914-633-2638; Email: SLee@iona.edu

# **Authors**

Escarlin Perez – Department of Chemistry and Biochemistry, Iona College, New Rochelle, New York 10801, United States Jasmin Ceja-Vega – Department of Chemistry and Biochemistry, Iona College, New Rochelle, New York 10801, United States

Michael Krmic – Department of Chemistry and Biochemistry, Iona College, New Rochelle, New York 10801, United States Alondra Gamez Hernandez – Department of Chemistry and Biochemistry, Iona College, New Rochelle, New York 10801, United States

Jamie Gudyka – Department of Chemistry and Biochemistry, Iona College, New Rochelle, New York 10801, United States Riley Porteus – Department of Chemistry and Biochemistry, Iona College, New Rochelle, New York 10801, United States

Complete contact information is available at: https://pubs.acs.org/10.1021/acschemneuro.2c00040

## **Author Contributions**

E.P. and A.G. have performed the differential scanning calorimetry experiment; J.C.-V. and J.G. have performed the water permeability experiment; M.K. and R.P. have performed the interfacial tension experiment; S.L. supervised the project and wrote the manuscript.

# **Funding**

This work was supported by the National Science Foundation (NSF-CHE-2002900 and NSF-DUE-1643737) and Iona College.

# Notes

The authors declare no competing financial interest.

#### ACKNOWLEDGMENTS

E.P. and A.G. are NSF S-STEM scholarship recipients and grateful for the research support in part through the NSF S-STEM program. E.P. is a Clare Boothe Luce Research Scholar and is grateful for the Henry Luce Foundation for the support in part.

## REFERENCES

- (1) Nelson, K. M.; Bisson, J.; Singh, G.; Graham, J. G.; Chen, S.-N.; Friesen, J. B.; Dahlin, J. L.; Niemitz, M.; Walters, M. A.; Pauli, G. F. The essential medicinal chemistry of cannabidiol (CBD). *J. Med. Chem.* **2020**, *63*, 12137–12155.
- (2) Peng, H.; Shahidi, F. Cannabis and cannabis edibles: A review. J. Agric. Food Chem. 2021, 69, 1751–1774.
- (3) Millar, S. A.; Stone, N. L.; Yates, A. S.; O'sullivan, S. E. A systematic review on the pharmacokinetics of cannabidiol in humans. *Front. Pharmacol.* **2018**, *9*, 1365.
- (4) Ramalho, Ì. M. D. M.; Pereira, D. T.; Galvão, G. B. L.; Freire, D. T.; Amaral-Machado, L.; Alencar, E. D. N.; Egito, E. S. T. D. Current

- trends on cannabidiol delivery systems: where are we and where are we going? Expert Opin. Drug Delivery 2021, 18, 1577-1587.
- (5) Devinsky, O.; Cross, J. H.; Laux, L.; Marsh, E.; Miller, I.; Nabbout, R.; Scheffer, I. E.; Thiele, E. A.; Wright, S. Trial of cannabidiol for drug-resistant seizures in the Dravet syndrome. *N. Engl. J. Med.* **2017**, *376*, 2011–2020.
- (6) McGuire, P.; Robson, P.; Cubala, W. J.; Vasile, D.; Morrison, P. D.; Barron, R.; Taylor, A.; Wright, S. Cannabidiol (CBD) as an adjunctive therapy in schizophrenia: a multicenter randomized controlled trial. *Am. J. Psychiatry* **2018**, *175*, 225–231.
- (7) Cristino, L.; Bisogno, T.; Di Marzo, V. Cannabinoids and the expanded endocannabinoid system in neurological disorders. *Nat. Rev. Neurol.* **2020**, *16*, 9–29.
- (8) Devinsky, O.; Cilio, M. R.; Cross, H.; Fernandez-Ruiz, J.; French, J.; Hill, C.; Katz, R.; Di Marzo, V.; Jutras-Aswad, D.; Notcutt, W. G.; Martinez-Orgado, J.; Robson, P. J.; Rohrback, B. G.; Thiele, E. A.; Whalley, B. J.; Friedman, D. Cannabidiol: pharmacology and potential therapeutic role in epilepsy and other neuropsychiatric disorders. *Epilepsia* **2014**, *55*, 791–802.
- (9) Blaskovich, M. A.; Kavanagh, A. M.; Elliott, A. G.; Zhang, B.; Ramu, S.; Amado, M.; Lowe, G. J.; Hinton, A. O.; Zuegg, J.; Beare, N.; Quach, D.; Sharp, M. D.; Pogliano, J.; Robgers, A. P.; Lyras, D.; Tan, L.; West, N. P.; Crawford, D. W.; Peterson, M. L.; Callahan, M.; Thurn, M. The antimicrobial potential of cannabidiol. *Commun. Biol.* **2021**, *4*, 1–18.
- (10) Seltzer, E. S.; Watters, A. K.; MacKenzie, D.; Granat, L. M.; Zhang, D. Cannabidiol (CBD) as a promising anti-cancer drug. *Cancers* **2020**, *12*, 3203.
- (11) Mangal, N.; Erridge, S.; Habib, N.; Sadanandam, A.; Reebye, V.; Sodergren, M. H. Cannabinoids in the landscape of cancer. *J. Cancer Res. Clin. Oncol.* **2021**, *147*, 2507–2534.
- (12) Watkins, A. R. Cannabinoid interactions with ion channels and receptors. *Channels* **2019**, *13*, 162–167.
- (13) Ghovanloo, M.-R.; Ruben, P. C. Cannabidiol and Sodium Channel Pharmacology: General Overview, Mechanism, and Clinical Implications. *Neuroscientist* **2021**, No. 10738584211017009.
- (14) Bragança, V. A.; França, T. G.; de Jesus, A. C.; Palheta, I. C.; Melo, F. P.; Neves, P. A.; Lima, A. B.; Borges, R. S. Impact of conformational and solubility properties on psycho-activity of cannabidiol (CBD) and tetrahydrocannabinol (THC). *Chem. Data Collect.* 2020, 26, No. 100345.
- (15) Bih, C. I., Chen, T.; Nunn, A. V.; Bazelot, M.; Dallas, M.; Whalley, B. J. Molecular targets of cannabidiol in neurological disorders. *Neurotherapeutics* **2015**, *12*, 699–730.
- (16) Ghovanloo, M.-R.; Choudhury, K.; Bandaru, T. S.; Fouda, M. A.; Rayani, K.; Rusinova, R.; Phaterpekar, T.; Nelkenbrecher, K.; Watkins, A. R.; Poburko, D.; Thewalt, J.; Andersen, O. S.; Delemotte, L.; Goodchild, S. J.; Ruben, P. C. Cannabidiol inhibits the skeletal muscle Nav1. 4 by blocking its pore and by altering membrane elasticity. *J. Gen. Physiol.* **2021**, *153*, No. e202012701.
- (17) Andersen, O. S.; Koeppe, R. E. Bilayer thickness and membrane protein function: an energetic perspective. *Annu. Rev. Biophys. Biomol. Struct.* **200**7, *36*, 107–130.
- (18) Phillips, R.; Ursell, T.; Wiggins, P.; Sens, P. Emerging roles for lipids in shaping membrane-protein function. *Nature* **2009**, *459*, 379–385.
- (19) Ingólfsson, H. I.; Thakur, P.; Herold, K. F.; Hobart, E. A.; Ramsey, N. B.; Periole, X.; De Jong, D. H.; Zwama, M.; Yilmaz, D.; Hall, K.; Maretzky, T.; Hemmings, J.; Hugh, C.; Blobel, C.; Marrink, S. J.; Kocer, A.; Sack, J. T.; Andersen, O. S. Phytochemicals perturb membranes and promiscuously alter protein function. *ACS Chem. Biol.* **2014**, *9*, 1788–1798.
- (20) Lawrence, D.; Gill, E. The effects of  $\Delta 1$ -tetrahydrocannabinol and other cannabinoids on spin-labeled liposomes and their relationship to mechanisms of general anesthesia. *Mol. Pharmacol.* 1975, 11, 595–602.
- (21) Bach, D.; Raz, A.; Goldman, R. The effect of hashish compounds on phospholipid phase transition. *Biochim. Biophys. Acta, Biomembr.* **1976**, 436, 889–894.

- (22) Tamir, I.; Lichtenberg, D.; Mechoulam, R. Interaction of cannabinoids with model membranes—nmr studies. In *Nuclear Magnetic Resonance Spectroscopy in Molecular Biology*; Springer, 1978; pp 405–422.
- (23) Hillard, C.; Harris, R.; Bloom, A. Effects of the cannabinoids on physical properties of brain membranes and phospholipid vesicles: fluorescence studies. *J. Pharmacol. Exp. Ther.* **1985**, 232, 579–588.
- (24) Yeagle, P. Modulation of membrane function by cholesterol. *Biochimie* **1991**, *73*, 1303–1310.
- (25) Ohvo-Rekilä, H.; Ramstedt, B.; Leppimäki, P.; Slotte, J. P. Cholesterol interactions with phospholipids in membranes. *Prog. Lipid Res.* **2002**, *41*, 66–97.
- (26) Lundbæk, J. A.; Birn, P.; Hansen, A. J.; Søgaard, R.; Nielsen, C.; Girshman, J.; Bruno, M. J.; Tape, S. E.; Egebjerg, J.; Greathouse, D. V. Regulation of Sodium Channel Function by Bilayer Elasticity The Importance of Hydrophobic Coupling. Effects of Micelle-forming Amphiphiles and Cholesterol. *J. Gen. Physiol.* **2004**, *123*, 599–621.
- (27) Dietschy, J. M. Central nervous system: cholesterol turnover, brain development and neurodegeneration. *Biol. Chem.* **2009**, 390, 287–293.
- (28) Yao, L.; Wells, M.; Wu, X.; Xu, Y.; Zhang, L.; Xiong, W. Membrane cholesterol dependence of cannabinoid modulation of glycine receptor. *FASEB J.* **2020**, *34*, 10920–10930.
- (29) Martin, L. J.; Banister, S. D.; Bowen, M. T. Understanding the complex pharmacology of cannabidiol: Mounting evidence suggests a common binding site with cholesterol. *Pharmacol. Res.* **2021**, *166*, No. 105508.
- (30) Sievers, M. H.; D'Alessandro, A.; Liu, X.; William, M. Multi-Omic Analysis Reveals Disruption of Cholesterol Homeostasis by Cannabidiol in Human Cell Lines. *bioRxiv* **2020**, No. 130864.
- (31) Ding, X.; Zhang, W.; Li, S.; Yang, H. The role of cholesterol metabolism in cancer. Am. J. Cancer Res. 2019, 9, 219.
- (32) Allen, J. A.; Halverson-Tamboli, R. A.; Rasenick, M. M. Lipid raft microdomains and neurotransmitter signalling. *Nat. Rev. Neurosci.* **2007**, *8*, 128–140.
- (33) Korade, Z.; Kenworthy, A. K. Lipid rafts, cholesterol, and the brain. *Neuropharmacology* **2008**, *55*, 1265–1273.
- (34) Van Meer, G.; Voelker, D. R.; Feigenson, G. W. Membrane lipids: where they are and how they behave. *Nat. Rev. Mol. Cell Biol.* **2008**, *9*, 112–124.
- (35) Rosilio, V. How can artificial lipid models mimic the complexity of molecule—membrane interactions? In *Advances in Biomembranes and Lipid Self-Assembly*; Elsevier, 2018; Vol. 27, pp 107–146.
- (36) Funakoshi, K.; Suzuki, H.; Takeuchi, S. Lipid bilayer formation by contacting monolayers in a microfluidic device for membrane protein analysis. *Anal. Chem.* **2006**, *78*, 8169–8174.
- (37) Holden, M. A.; Needham, D.; Bayley, H. Functional bionetworks from nanoliter water droplets. *J. Am. Chem. Soc.* **2007**, 129, 8650–8655.
- (38) De Wit, G.; Danial, J. S.; Kukura, P.; Wallace, M. I. Dynamic label-free imaging of lipid nanodomains. *Proc. Natl. Acad. Sci. U. S. A.* **2015**, *112*, 12299–12303.
- (39) Taylor, G. J.; Heberle, F. A.; Seinfeld, J. S.; Katsaras, J.; Collier, C. P.; Sarles, S. A. Capacitive detection of low-enthalpy, higher-order phase transitions in synthetic and natural composition lipid membranes. *Langmuir* **2017**, *33*, 10016–10026.
- (40) Punnamaraju, S.; Steckl, A. J. Voltage control of droplet interface bilayer lipid membrane dimensions. *Langmuir* **2011**, *27*, 618–626.
- (41) Huang, J.; Lein, M.; Gunderson, C.; Holden, M. A. Direct quantitation of peptide-mediated protein transport across a droplet—interface bilayer. *J. Am. Chem. Soc.* **2011**, *133*, 15818–15821.
- (42) Najem, J. S.; Dunlap, M. D.; Rowe, I. D.; Freeman, E. C.; Grant, J. W.; Sukharev, S.; Leo, D. J. Activation of bacterial channel MscL in mechanically stimulated droplet interface bilayers. *Sci. Rep.* **2015**, *5*, 13726.
- (43) Villar, G.; Graham, A. D.; Bayley, H. A tissue-like printed material. *Science* **2013**, *340*, 48–52.

- (44) Michalak, Z.; Fartash, D.; Haque, N.; Lee, S. Tunable crystallization via osmosis-driven transport across a droplet interface bilayer. *CrystEngComm* **2012**, *14*, 7865–7868.
- (45) Michalak, Z.; Muzzio, M.; Milianta, P. J.; Giacomini, R.; Lee, S. Effect of monoglyceride structure and cholesterol content on water permeability of the droplet bilayer. *Langmuir* **2013**, *29*, 15919–15925.
- (46) Milianta, P. J.; Muzzio, M.; Denver, J.; Cawley, G.; Lee, S. Water permeability across symmetric and asymmetric droplet interface bilayers: interaction of cholesterol sulfate with DPhPC. *Langmuir* **2015**, *31*, 12187–12196.
- (47) Zeidel, M. L. Water homeostasis: evolutionary medicine. *Trans. Am. Clin. Climatol. Assoc.* **2012**, 123, 93.
- (48) Shinoda, K.; Shinoda, W.; Mikami, M. Efficient free energy calculation of water across lipid membranes. *J. Comput. Chem.* **2008**, 29, 1912–1918.
- (49) MacAulay, N. Molecular mechanisms of brain water transport. *Nat. Rev. Neurosci.* **2021**, *22*, 326–344.
- (50) Hill, W. G.; Zeidel, M. L. Reconstituting the Barrier Properties of a Water-tight Epithelial Membrane by Design of Leaflet-specific Liposomes\* 210. *J. Biol. Chem.* **2000**, 275, 30176–30185.
- (51) Lopez, M.; Evangelista, S. E.; Morales, M.; Lee, S. Enthalpic effects of chain length and unsaturation on water permeability across droplet bilayers of homologous monoglycerides. *Langmuir* **2017**, *33*, 900–912.
- (52) Lopez, M.; Denver, J.; Evangelista, S. E.; Armetta, A.; Di Domizio, G.; Lee, S. Effects of Acyl Chain Unsaturation on Activation Energy of Water Permeability across Droplet Bilayers of Homologous Monoglycerides: Role of Cholesterol. *Langmuir* **2018**, *34*, 2147–2157.
- (53) Lee, S. Good to the last drop: interfacial droplet chemistry, from crystals to biological membranes. *Acc. Chem. Res.* **2018**, *51*, 2524–2534.
- (54) Foley, S.; Miller, E.; Braziel, S.; Lee, S. Molecular organization in mixed SOPC and SDPC model membranes: Water permeability studies of polyunsaturated lipid bilayers. *Biochim. Biophys. Acta, Biomembr.* **2020**, *1862*, No. 183365.
- (55) Wood, M.; Morales, M.; Miller, E.; Braziel, S.; Giancaspro, J.; Scollan, P.; Rosario, J.; Gayapa, A.; Krmic, M.; Lee, S. Ibuprofen and the Phosphatidylcholine Bilayer: Membrane Water Permeability in the Presence and Absence of Cholesterol. *Langmuir* **2021**, *37*, 4468–4480.
- (56) Ingólfsson, H. I.; Carpenter, T. S.; Bhatia, H.; Bremer, P.-T.; Marrink, S. J.; Lightstone, F. C. Computational lipidomics of the neuronal plasma membrane. *Biophys. J.* **2017**, *113*, 2271–2280.
- (57) Calapai, F.; Cardia, L.; Sorbara, E. E.; Navarra, M.; Gangemi, S.; Calapai, G.; Mannucci, C. Cannabinoids, Blood—Brain Barrier, and Brain Disposition. *Pharmaceutics* **2020**, *12*, 265.
- (58) Mouritsen, O. G.; Jørgensen, K. Dynamical order and disorder in lipid bilayers. *Chem. Phys. Lipids* **1994**, *73*, 3–25.
- (59) Mathai, J. C.; Tristram-Nagle, S.; Nagle, J. F.; Zeidel, M. L. Structural determinants of water permeability through the lipid membrane. *Gen. Physiol.* **2008**, *131*, 69–76.
- (60) Alwarawrah, M.; Dai, J.; Huang, J. A molecular view of the cholesterol condensing effect in DOPC lipid bilayers. *J. Phys. Chem. B* **2010**, *114*, 7516–7523.
- (61) Jurak, M.; Chibowski, E. Characteristics of a phospholipid DOPC/cholesterol bilayer based on surface free energy and its components. *RSC Adv.* **2015**, *5*, 66628–66635.
- (62) Boughter, C. T.; Monje-Galvan, V.; Im, W.; Klauda, J. B. Influence of cholesterol on phospholipid bilayer structure and dynamics. *J. Phys. Chem. B* **2016**, 120, 11761–11772.
- (63) Olbrich, K.; Rawicz, W.; Needham, D.; Evans, E. Water permeability and mechanical strength of polyunsaturated lipid bilayers. *Biophys. J.* **2000**, *79*, 321–327.
- (64) Stubbs, C. D.; Smith, A. D. The modification of mammalian membrane polyunsaturated fatty acid composition in relation to membrane fluidity and function. *Biochim. Biophys. Acta, Rev. Biomembr.* **1984**, 779, 89–137.

- (65) Koynova, R.; Caffrey, M. Phases and phase transitions of the phosphatidylcholines. *Biochim. Biophys. Acta, Rev. Biomembr.* **1998**, 1376, 91–145.
- (66) Bach, D.; Sela, B. Thermotropic properties of calf-brain lipids interacting with drugs—II. *Biochem. Pharmacol.* **1981**, *30*, 1777—1780.
- (67) Jørgensen, K.; Ipsen, J. H.; Mouritsen, O. G.; Bennett, D.; Zuckermann, M. J. A general model for the interaction of foreign molecules with lipid membranes: drugs and anaesthetics. *Biochim. Biophys. Acta, Biomembr.* 1991, 1062, 227–238.
- (68) Davis, P.; Keough, K. Differential scanning calorimetric studies of aqueous dispersions of mixtures of cholesterol with some mixed-acid and single-acid phosphatidylcholines. *Biochemistry* **1983**, 22, 6334–6340.
- (69) Fritzsching, K. J.; Kim, J.; Holland, G. P. Probing lipid—cholesterol interactions in DOPC/eSM/Chol and DOPC/DPPC/Chol model lipid rafts with DSC and 13C solid-state NMR. *Biochim. Biophys. Acta, Biomembr.* **2013**, 1828, 1889—1898.
- (70) Huang, J.; Feigenson, G. W. A microscopic interaction model of maximum solubility of cholesterol in lipid bilayers. *Biophys. J.* **1999**, 76, 2142–2157.
- (71) Chapnick, D.; Liu, X.; Old, W. Novel Systems And Methods For The Therapeutic Use of Cannabinoids or Cannabinoid Analogs to Increase The Lipid Order of Cholesterol Containing Cell Membranes. US-2021/0244686-A1, 2021.
- (72) Marsh, D. Lateral pressure in membranes. *Biochim. Biophys. Acta, Rev. Biomembr.* **1996**, 1286, 183–223.
- (73) Cantor, R. S. Lipid composition and the lateral pressure profile in bilayers. *Biophys. J.* **1999**, *76*, 2625–2639.
- (74) Cantor, R. S. The lateral pressure profile in membranes: a physical mechanism of general anesthesia. *Biochemistry* **1997**, *36*, 2339–2344.
- (75) Perozo, E.; Kloda, A.; Cortes, D. M.; Martinac, B. Physical principles underlying the transduction of bilayer deformation forces during mechanosensitive channel gating. *Nat. Struct. Biol.* **2002**, *9*, 696–703.
- (76) Nomura, T.; Cranfield, C. G.; Deplazes, E.; Owen, D. M.; Macmillan, A.; Battle, A. R.; Constantine, M.; Sokabe, M.; Martinac, B. Differential effects of lipids and lyso-lipids on the mechanosensitivity of the mechanosensitive channels MscL and MscS. *Proc. Natl. Acad. Sci. U. S. A.* **2012**, *109*, 8770–8775.
- (77) Faugeras, V.; Duclos, O.; Bazile, D.; Thiam, A. R. Membrane determinants for the passive translocation of analytes through droplet interface bilayers. *Soft Matter* **2020**, *16*, 5970–5980.
- (78) Taylor, G. J.; Venkatesan, G. A.; Collier, C. P.; Sarles, S. A. Direct in situ measurement of specific capacitance, monolayer tension, and bilayer tension in a droplet interface bilayer. *Soft Matter* **2015**, *11*, 7592–7605.
- (79) Wilson, K. A.; MacDermott-Opeskin, H. I.; Riley, E.; Lin, Y.; O'Mara, M. L. Understanding the link between lipid diversity and the biophysical properties of the neuronal plasma membrane. *Biochemistry* **2020**, *59*, 3010–3018.
- (80) Paula, S.; Volkov, A.; Van Hoek, A.; Haines, T.; Deamer, D. W. Permeation of protons, potassium ions, and small polar molecules through phospholipid bilayers as a function of membrane thickness. *Biophys. J.* **1996**, *70*, 339–348.